Gold-Catalyzed Synthesis of Aromatic Azo Compounds from Anilines and Nitroaromatics

REPORTS

Gold-Catalyzed Synthesis of Aromatic Azo Compounds from Anilines and Nitroaromatics

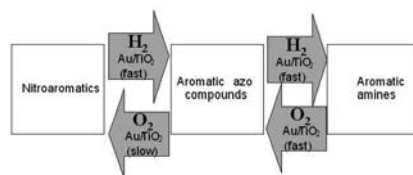Abdessamad Grirrane, Avelino Corma,* Hermenegildo García*

The selective formation of aromatic azo compounds at preparative or industrial levels requires stoichiometric amounts of environmentally unfriendly transition metals or nitrites. Here, we show that gold nanoparticles supported on titanium dioxide (TiO_2) and nanoparticulated cerium dioxide (CeO_2) catalyze the aerobic oxidation of aromatic anilines to aromatic azo compounds with yields above 98% under mild reaction conditions. Gold on TiO_2 can also act as a reductive catalyst to access the compound directly from nitroaromatics through a two-step, one-pot reaction. The catalytic process shows promise for efficient synthesis of symmetric aromatic azo compounds, and even a range of asymmetric aromatic azo compounds.

Aromatic azo compounds are high-value chemicals widely used in industry as dyes, pigments, food additives, and drugs (1–3). They are obtained either by reduction of nitroaromatics or by oxidation of anilines. Despite their importance, however, no current catalytic route offers high yields and selectivities. Therefore, the preparation of aromatic azo compounds is carried out today using stoichiometric reagents and, frequently, environmentally unfriendly transition metals (4). Examples include oxidation of aromatic amines with lead tetraacetate (5) and reduction of nitroaromatics with lead metal (6, 7). An alternative route to asymmetrically substituted aromatic azo compounds entails coupling of diazonium salts with electron-rich aromatic compounds (8). This process requires stoichiometric amounts of nitrite salts to form the diazonium salt and generates equivalent amounts of inorganic salt waste. A previous report on the catalytic oxidation of aniline with hydrogen peroxide using microporous crystalline titanosilicate TS-1 shows minimal azobenzene formation, instead noting nitrosobenzene and azoxybenzene products (9).

A sustainable chemical process for highly selective synthesis of aromatic azo compounds is thus of great fundamental as well as practical interest. We demonstrate such a process here with an environmentally benign catalyst for oxidation of anilines by oxygen under mild reaction conditions, with yields above 98%.

We recently discovered that gold on TiO_2 (Au/TiO_2) is an excellent catalyst for the chemoselective reduction of nitroaromatics to anilines (10). The key to this process is the capacity of the metal to induce H_2 dissociation and the specific conformation of the adsorbed nitroaromatic reactant at the interface between the nanoparticles of gold and the TiO_2 support (11). According to Haber's mechanism (11), one route for hydrogenation of nitrobenzene to aniline takes place through bimolecular coupling of aniline and nitrosobenzene, forming azo benzene as intermediate, which is subsequently rapidly hydrogenated to two anilines (Scheme 1). The intermediacy of the azo compound in the selective hydrogenation of nitroaromatics, when occuring through the above route, was sup-

ported by performing the hydrogenation of azobenzene in the presence of Au/TiO_2 and observing the formation of aniline (10). Taking into account the principle of microscopic reversibility and considering that the azo compound is more difficult to oxidize than aniline, we were motivated to explore gold nanoparticles supported on TiO_2 as catalyst for the oxidation of anilines to the corresponding aromatic azo compounds (Scheme 1).

On the basis of this hypothesis we exposed aniline to gold nanoparticles on TiO_2 (Au/TiO_2) under mild aerobic oxidation conditions, i.e., 3 to 5 bars of oxygen pressure at 100°C (12), and observed selective conversion to the corresponding azobenzenes (Fig. 1 and Table 1).

Control experiments showed that thermal oxidation of aniline does not occur, and the TiO_2 support alone induced significantly lower conversion, indicating that gold plays an important role in the catalytic process (fig. S1). Moreover, to produce active Au/TiO_2 catalysts, the gold must be prepared in the form of nanometer-scale crystallites. When the average size of the gold nanoparticles is increased from 4 to 25 nm, the activity of the catalyst strongly decreases (Table 1).

As observed with other gold-catalyzed processes (13), the nature of the support has a strong influence on the activity of the gold nanoparticles. Whereas gold nanoparticles on TiO_2 proved active and selective catalysts for formation of azobenzene, gold with similar crystallite size on carbon or ferric oxide was not active. Gold supported on nanocrystalline ceria is an active and
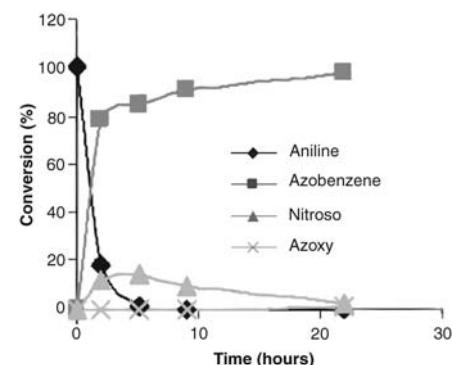
Scheme 1.

Fig. 1. Time-conversion plot for aniline oxidation, 1.5% Au/TiO_2, 100°C. For reaction conditions, see Table 1.

1661

Downloaded from www.sciencemag.org on December 12, 2008

selective catalyst for the aerobic oxidation of alcohols (14), and it also showed excellent activity and selectivity for formation of azobenzene (Table 1).

We furthermore found that gold is uniquely active for aniline oxidation compared with other noble metals (Table 1 and fig. S1). Our attempts to oxidize aniline to azobenzene with titania- or carbon-supported palladium or platinum nanoparticles under the same reaction conditions were unsuccessful. We also found no catalytic improvement when using, instead of Au/TiO_2 core-shell gold nanoalloys, Au(core)-Pd(shell)/TiO_2 whose preparation and properties have been recently reported (15). In addition, Au behaves differently from Pd and Pt (Table 1). These observations can be attributed to the higher affinity of Pd and Pt for amine adsorption, which blocks their activity relative to Au.

Having established that Au/TiO_2 is able to catalyze both the aerobic oxidation of anilines to azobenzenes and the chemoselective hydrogenation of nitroaromatics to anilines (10), we explored coupling these two reactions in a single-pot process to transform nitrobenzenes into aromatic azo compounds (Scheme 1). We hydrogenated nitrobenzene to aniline with the Au/TiO_2 catalyst and then, after flushing out the H_2, admitted oxygen at 5 bar into the reaction system (12). The results presented in Table 2 show that it is possible to achieve high conversion of nitrobenzene with excellent selectivity to azobenzene through this one-pot procedure.
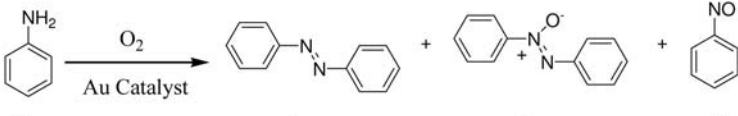
The general applicability of the catalytic oxidation was tested with a series of substituted anilines (Table 3). The reaction was remarkably selective for azobenzene product regardless of the presence of electron donor or acceptor substituents. The reaction rate depended qualitatively on the Hammett σ constant of the substituent, oxidation being favored by the presence of electron donor substituents. The food additive "butter yellow" can be catalytically synthesized in excellent yield starting from N,N-dimethylaniline (Table 3).

Beyond symmetrically substituted azobenzenes, azo dyes composed of two different aromatic rings—one electron-rich and the other electron-poor—constitute an industrially important class of compounds. As noted earlier, these azo dyes are typically synthesized through coupling of the diazonium salt of the electron-poor partner with the electron-rich arene (8). Considering the influence of ring substitution on the reaction rate, we thought that the Au catalytic coupling could also be successfully applied to the preparation of these asymmetric aromatic azo dyes by reacting a mixture of the two different anilines directly, provided that one partner proved much more reactive than the other. Our expectation was realized, and we were able to obtain several asymmetrically substituted azobenzenes of industrial interest (Table 4), including methyl orange dye at high selectivity and conversion, using the Au/TiO_2 catalyst.
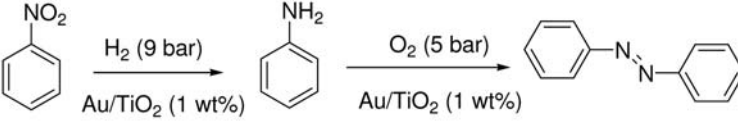
A reasonable reaction mechanism for the catalytic process would involve as the first step a single-electron oxidation of aniline to the corresponding radical cation, mediated by the TiO_2-supported gold nanoparticles through unsaturated gold sites and/or $Au^{\delta+}$ species formed by interaction with the support (Scheme 2). This mechanism takes into account the higher gold oxidation potential in comparison to palladium or platinum.

We obtained electron paramagnetic resonance data to support the occurrence of this first electron transfer step. Using N-tert-butyl-α-phenylnitrone as a trapping agent, we were able to confirm the formation of aniline radical cation when a solution of aniline in toluene is stirred at room temperature in the presence of 1.5 weight percent (wt %) Au/TiO_2 (fig. S2). The measured spectrum matched a simulated spectrum for the trapped anilinium cation structure.

Table 1. Results of the aerobic oxidation of aniline (1a) in the presence of supported metal nanoparticles as catalyst. Reaction conditions: Preheated anilines (93, 13 mg) at 100°C dissolved in toluene (2 ml), stirred magnetically in a reinforced glass vial (3 ml) at an initial O_2 pressure of 5 bar in the presence of the solid catalyst (metal/aniline mol ratio 1%). *, Unidentified product accounts for 10.5%; †, Unidentified product accounts for 11.5%.

Catalyst	Time (h)	Yield (%) 2a	Yield (%) 3a	Yield (%) 4a	Conv. (%)	Selectivity (%)
1.5 % Au/TiO_2	9	90	0	10	100	90
	22	98	0.5	1.5	100	98
1.5 % Au/TiO_2 (reused catalyst)	22	99	0	0	100	99
TiO_2	24	52.5	0	0.5	53	99
1.5 % Au/TiO_2 (Particle size 25 nm)	30	4.5	0	0	4,5	99
0.5 % Fe/TiO_2	7	61	0	1	62	98
	24	83.5	0.5	2.5	95	96.5
Au(1.5%)Pd(0.8%)/TiO_2	34	8.4	0	0	8.4	99
Au(1.5%)Pd(1.8%)/TiO_2	23	No reaction				
5 % Pd/TiO_2	35	No reaction				
4.4 % Au/Fe_2O_3	47	No reaction				
0.8 % Au/C	69	No reaction				
5 % Pd/C	80	No reaction				
0.2 % Pt/C	40	No reaction				
5 % Pt/TiO_2	70	No reaction				
0.44 % Au/CeO_2	6	91	7	0	98	91
	10	93	7	0	100	93
Au(0.44%)Pd(10.15%)/CeO_2	20	83	6.5	0*	100	83
CeO_2	42	59	19.5	0†	90	59

Table 2. Synthesis of azobenzene from nitrobenzene through a two-step, one-pot process.

Catalyst	T °C	P (bar)	Time (h)	Yield (%)	Conversion (%)	Selectivity (%)
1.5 % Au/TiO_2	120 °C	H_2 (9 bar)	6	94.6 Aniline	98.5	96
	100 °C	O_2 (5 bar)	9	92 Azobenzene	100	92

As shown in Scheme 2, the single-electron abstraction would be followed by the coupling of aniline radical cation with neutral aniline to form a three-electron sigma bond. This reaction step is supported by many published precedents for the general tendency of amine radical cations to form N-N bonds that can eventually lead to hydrazines by consecutive losses of two protons and one electron (16–20).

Once formed, hydrazines should be even more easily oxidized than the parent amine and thus quickly converted to the corresponding azobenzene, following a pathway that again involves alternating transfer of electrons and protons. To support the possibility of this reaction step, we carried out the oxidation of diphenylhydrazine by oxygen in the presence of Au/TiO₂ under the same reaction conditions used for aniline oxidation. We observed that diphenylhydrazine was converted to azobenzene at least 10 times as fast as aniline, as could be expected based on their general relative reactivity. This result explains why we failed to detect hydrazine as an intermediate during aniline oxidation. Under the reaction mechanism proposed in Scheme 2, oxygen serves as the final sink of the electrons, giving rise to the formation of two water molecules.

The mechanism outlined in Scheme 2 could be operating simultaneously with another having nitrosobenzene as a key intermediate. There are precedents for nitrosobenzene reaction with aniline to yield azobenzene as the final product (21). The fact that nitrosobenzene 4 has been detected in minor quantities during the course of the initial stages of the reaction lends support to this possibility.

On the basis of the proposed main reaction pathway, we can rationalize that a solid with defect sites or vacancies able to abstract an electron from aniline, as well as to activate oxygen, should catalyze the reaction. In this context, increasing the number of vacancies or defect sites on the TiO₂ surface by doping with iron (12, 22) should enhance the reaction further. Indeed we found that the resulting Fe-TiO₂ material exhibits higher activity than TiO₂ for the formation of azobenzene, whereas Fe₂O₃ is not active (Table 1 and fig. S1).

From the results of the present study and on the basis of the proposed major mechanism, it should be possible to develop a wide array of solid catalysts for the conversion of aromatic amines to azo compounds, provided that enough defect sites are generated on the surface. However, among them, Au/TiO₂ not only gives the highest selectivity of the materials tested here but also should allow the efficient one-pot conversion of a wide range of nitroaromatics into azo compounds.
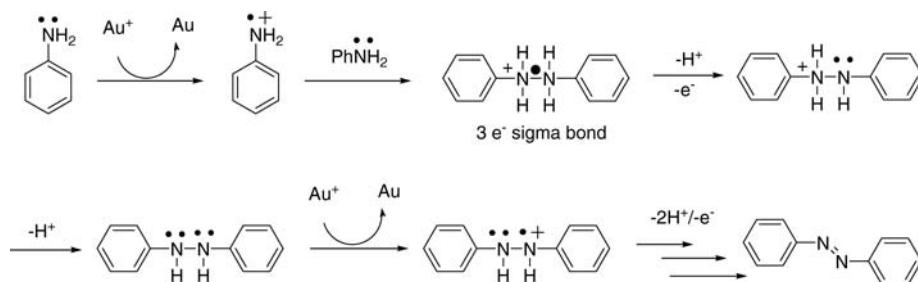
Table 3. Results of the aerobic oxidation of anilines 1b-f in the presence of supported metal nanoparticles as catalyst. Reaction conditions: Preheated anilines (93, 13 mg) at 100°C dissolved in toluene (2 ml), stirred magnetically in a reinforced glass vial (3 ml) at an initial O₂ pressure of 5 bar in the presence of the solid catalyst (metal/aniline mol ratio 1%). *, 3-bar oxygen pressure.

R	Catalyst	Time (h)	Yield 2	Yield 3	Yield 4	Conversion (%)	Selectivity (%)
OCH₃*	1.5 wt% Au/TiO₂	5	89	3	6	99	90
CH₃	1.5 wt% Au/TiO₂	3	98	0	2	99	98
Cl	1.5 wt% Au/TiO₂	23	64	0	0	65	99
COCH₃	1.5 wt% Au/TiO₂	31	44	1	0.5	50	96
N(CH₃)₂	1.5 wt% Au/TiO₂	16	99	0	0	99	99

Table 4. Results of the aerobic oxidation of an equimolar mixture of substituted aromatic amines in the presence of 1.5 wt % Au/TiO₂ (1 mol %) as catalyst for the formation of asymmetrically substituted azobenzenes. Reaction conditions: Toluene, 100°C, 5 bar O₂. *, Based on p-R^{1}C₆H₄NH₂; †, Mixtures from two products derived from p-R^{1}C₆H₄NH₂ and p-R^{2}C₆H₄NH₂; ‡, Same reaction conditions using a 1:2 stoichiometry for p-toluidin versus 4-aminoacetophenone.

Substrates R¹	Substrates R²	Time (h)	Conversion (%)*	Selectivity (%) Azobenzenes Asymmetric	Selectivity (%) Azobenzenes Symmetric†	Nitrosobenzenes†	Azoxybenzenes†
CH₃	COCH₃	44	100	80	9	1	6
CH₃‡	COCH₃	43	87	90	5	2	1
N(CH₃)₂	SO₃Na	40	99	91			

3 e⁻ sigma bond

Scheme 2.

References and Notes
1. R. Egli, in *Colour Chemistry: The Design and Synthesis of Organic Dyes and Pigments*, A. P. Peter, H. S. Freeman, Eds. (Elsevier, London, 1991), chap. VII.
2. S. C. Catino, E. Farris, *Concise Encyclopedia of Chemical Technology* (Wiley, New York, 1985).
3. K. Venkataraman, in *The Chemistry of Synthetic Dyes* (Academic Press, London, 1970), chap. VI.
4. J. H. Clark, *Chemistry of Waste Minimization* (Chapman & Hall, London, 1995).
5. H. Firouzabadi, Z. Mostafavippor, *Bull. Chem. Soc. Jpn.* **56**, 914 (1983).
6. K. Ohe, S. Uemura, N. Sugita, H. Masuda, T. Taga, *J. Org. Chem.* **54**, 4169 (1989).
7. A. Osuka, H. Shimizu, H. Suzuki, *Chem. Lett.* **12**, 1373 (1983).
8. H. A. Dabbagh, A. Teimouri, A. N. Chermahini, *Dyes Pigments* **73**, 239 (2007).
9. S. Gontier, A. Tuel, *Appl. Catal. A* **118**, 173 (1994).
10. A. Corma, P. Serna, *Science* **313**, 332 (2006).
11. M. B. Smith, J. March, *Advanced Organic Chemistry*: I (Wiley, New York, ed. 5, 2001).

12. Materials and methods are available as supporting material on *Science* Online.
13. M. Haruta, *Catal. Today* **36**, 153 (1997).
14. A. Abad, P. Concepcion, A. Corma, H. Garcia, *Angew. Chem. Int. Ed.* **44**, 4066 (2005).
15. D. I. Enache *et al.*, *Science* **311**, 362 (2006).
16. J. C. Scaiano, S. García, H. García, *Tetrahedron Lett.* **38**, 5929 (1997).
17. O. Brede, A. Maroz, R. Hermann, S. Naumov, *J. Phys. Chem. A* **109**, 8081 (2005).
18. M. Oyama, M. Goto, *Indian J. Chem. Sect. A* **42A**, 733 (2003).
19. W. Hub, S. Schneider, F. Doerr, J. D. Oxman, F. D. Lewis, *J. Am. Chem. Soc.* **106**, 701 (1984).
20. W. Hub, S. Schneider, F. Doerr, J. D. Oxman, F. D. Lewis, *J. Phys. Chem.* **87**, 4351 (1983).
21. E. Lamy-Pitara, B. N' Zemba, J. Barbier, F. Barbot, L. Miginiac, *J. Mol. Catal. Al* **142**, 39 (1999).
22. S. Carrettin *et al.*, *Chem. Eur. J.* **13**, 7771 (2007).
23. Financial support by the Spanish DGI (MAT06-14274-C02-01 and CTQ2006-0658) is gratefully acknowledged. A.G. thanks the Spanish CSIC for a JAE research associate contract. A patent covering the use of these catalysts for the aerobic synthesis of azo benzenes has been filed at the Spanish Patent Office.

Collective Reactivity of Molecular Chains Self-Assembled on a Surface

Peter Maksymovych,[1,2] Dan C. Sorescu,[3] Kenneth D. Jordan,[1] John T. Yates Jr.[1,4]*

Self-assembly of molecules on surfaces is a route toward not only creating structures, but also engineering chemical reactivity afforded by the intermolecular interactions. Dimethyldisulfide (CH_3SSCH_3) molecules self-assemble into linear chains on single-crystal gold surfaces. Injecting low-energy electrons into individual molecules in the self-assembled structures with the tip of a scanning tunneling microscope led to a propagating chemical reaction along the molecular chain as sulfur–sulfur bonds were broken and then reformed to produce new CH_3SSCH_3 molecules. Theoretical and experimental evidence supports a mechanism involving electron attachment followed by dissociation of a CH_3SSCH_3 molecule and initiation of a chain reaction by one or both of the resulting CH_3S intermediates.

Self-assembled molecular structures on metal and semiconductor surfaces (*1*, *2*) can produce properties that are not observed in isolated adsorbed molecules. For example, the proximity of atoms or molecules can allow their electronic states to delocalize (*3–6*), leading to increased electron mobility in the overlayer that can be desirable for potential applications in molecular electronics and organic solar cells (*7*). Other functionalities that are enabled by self assembly include molecular cascades within prearranged molecules (*8*), directional polymerization (*9*), switching of electronic states of surface adatoms in molecular corrals (*10*), and the tunable confinement of electronic surface states in supramolecular gratings (*11*).
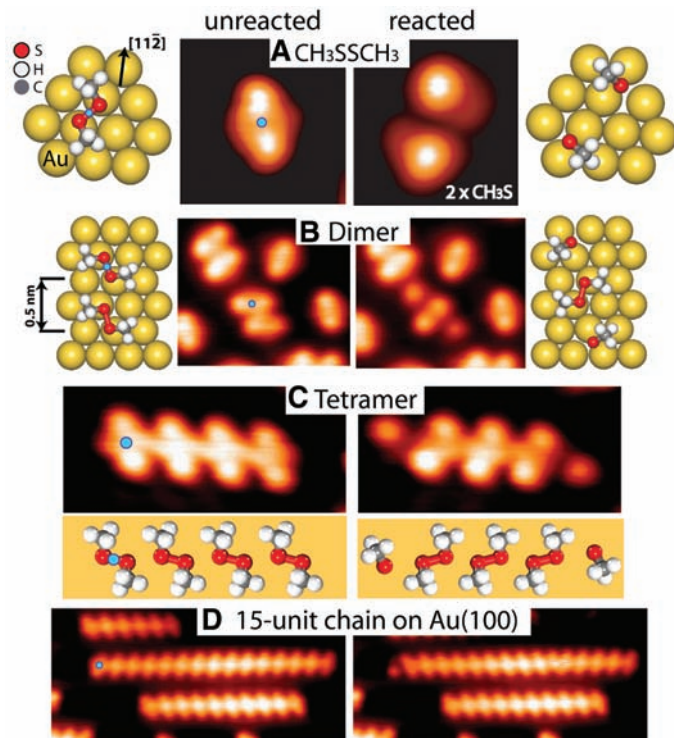
Here we report that chemical reactivity can also be induced by self-assembly. A linear chain of molecules (CH_3SSCH_3) adsorbed on a gold surface has been found to respond collectively to electron attachment and undergo a chemical reaction that involves S–S bond dissociation and recombination reactions extending throughout the molecular assembly. The molecular self-alignment reduces the activation energy to break the S–S bond of the CH_3SSCH_3 molecule inside the assembly by at least a factor of 5, allowing for the facile propagation of the chain reaction through as many as 10 neighboring molecules [on the Au(100) surface] before being quenched. The self-assembled molecular structure thus redirects the energy flow toward a chemical chain reaction involving multiple steps, rather than rapid dissipation into the metal bulk.

We have studied electron-induced reactions of CH_3SSCH_3 molecules bonded to Au(111) and Au(100) surfaces using scanning tunneling microscopy (STM) at 5 K to inject electrons and image the reaction products [see supporting online material (SOM)]. Single molecules adsorb on the Au(111) surface with a calculated binding energy of 11.8 kcal/mol in a structural geometry shown in Fig. 1A (*12*). Methyl groups located at the two ends of the S–S bond assume a trans conformation. We observed a total of six equivalent orientations of isolated CH_3SSCH_3 molecules (two mirror images for each of three azimuthal orientations) on the Au(111) surface. At a higher molecular coverage and at adsorption temperatures between 70 and 200 K, "linear" CH_3SSCH_3 chains up to five units in length form on the Au(111) surface. The epitaxial chains run along the $<11\bar{2}>$ crystallographic direction with a periodicity of 0.5 nm (Fig. 1, B and C). Every molecule in the chain has the same orientation of the S–S

[1]Department of Chemistry and Center for Molecular and Materials Simulations, University of Pittsburgh, Pittsburgh, PA 15260, USA. [2]Center for Nanophase Materials Sciences, Oak Ridge National Laboratory, Oak Ridge, TN 37831, USA. [3]U.S. Department of Energy, National Energy Technology Laboratory, Pittsburgh, PA 15236, USA. [4]Department of Chemistry, University of Virginia, Charlottesville, VA 22904, USA.

*To whom correspondence should be addressed. E-mail: johnt@virginia.edu

Fig. 1. STM images before and after electron-induced dissociation of a single CH_3SSCH_3 molecule and the self-assembled chains on the Au(111) surface. Schematic ball models of the selected structures are shown aside their STM images. (**A**) Dissociation of CH_3SSCH_3 producing two CH_3S fragments by a pulse of tunneling current at 1.4 V (*12*). (**B** and **C**) Chain reactions in CH_3SSCH_3 dimer and tetramer assemblies on Au(111) induced by a voltage pulse on top of the terminal molecule (blue dot, pulse voltage 0.9 V), leading to the synthesis of CH_3SSCH_3 molecules of opposite conformation. (**D**) A similar chain reaction on the Au(100) surface that involves 10 out of 15 molecules in a row and produces 9 new CH_3SSCH_3 molecules.